

# Deregulation of p27 and Cyclin D1/D3 Control Over Mitosis Is Associated with Unfavorable Prognosis in Non-small Cell Lung Cancer, as Determined in 405 Operated Patients

William Sterlacci, MD,\* Michael Fiegl, MD,† Wolfgang Hilbe, MD,† Herbert Jamnig, MD,‡ Wilhelm Oberaigner, MD,§ Thomas Schmid, MD,|| Florian Augustin, MD,|| Jutta Aubegger, MD,¶ Ellen C. Obermann, MD,# and Alexandar Tzankov, MD#

**Introduction:** A large group of interacting molecular factors, involved in epithelial-mesenchymal transition, epidermal growth factor receptor (EGFR) signaling, and G1 mitotic phase, are shown to play an important role in cancerogenesis and progression of non-small cell lung cancer (NSCLC). Since success concerning potential correlations, structural and numeric gene aberrations, and biological risk assessment of these molecular factors are still lacking, combined analysis of a multitude of intertwined factors is currently a promising approach.

**Methods:** Cyclins (D1, D2, D3, and E), p21, p27, EGFR, Snail, E-cadherin,  $\beta$ -catenin, phosphatidylinositol-3' kinase, phosphatase and tensin homologue, phosphorylated Akt, and phosphorylated signal transducer, and activator of transcription-3 were analyzed by immunohistochemistry in 405 surgically resected NSCLC, using a standardized tissue microarray platform. In addition, the gene status of EGFR and cyclin D1 was examined by fluorescence in situ hybridization. Extensive clinical data were acquired, enabling detailed clinicopathologic correlation during a postoperative follow-up period of up to 14 years.

**Results:** The protein overexpressions of nuclear p27, cyclin D1, cyclin D3, E-cadherin, and EGFR as assessed by immunohistochemistry were all associated with a significant reduction in overall

survival time. In addition, cyclin D1 proved especially important, being the only independent molecular tumor-related factor with prognostic significance by multivariable analysis. In analogy to EGFR, recurrent numeric gene aberrations, particularly high-level amplifications, of cyclin D1 were obvious.

**Conclusions:** The results emphasize that deregulation of controlling factors of the early G1 phase is of significant oncogenic relevance and may represent a potential treatment target in NSCLC.

**Key Words:** Non-small cell lung cancer, Cyclin D1, p27, EGFR, Epithelial-mesenchymal transition.

(*J Thorac Oncol.* 2010;5: 1325–1336)

The process of carcinoma progression to metastatic disease involves conversion of epithelial tumor cells into motile mesenchymal-like cells, which may then breach the underlying basal membrane, enter blood vessels, and spread to distant organs. This epithelial-mesenchymal transition (EMT) is a central step in tumor metastasis and has been associated with epidermal growth factor receptor (EGFR) signaling.<sup>1</sup> Expression of E-cadherin, a transmembrane glycoprotein localized mainly in adherent junctions is thereby down-regulated, which is associated with loss of cell-cell adherence.<sup>2</sup> Down-regulation of E-cadherin is considered as a critical step and an indicator for EMT, and it can be achieved by transcriptional suppression mediated by the transcription factors Snail, Slug, and Twist.<sup>3</sup> In cancer cells, activation of EGFR increases the abundance of Snail, which accumulates in the nucleus and suppresses the expression of E-cadherin.<sup>4</sup> E-cadherin is associated with a group of proteins called catenins ( $\alpha$ -,  $\beta$ -, and  $\gamma$ -catenin) and is directly bound to  $\beta$ -catenin, which also acts as a cytoplasmic signaling molecule when unbound. Reduction in E-cadherin leads to increased amounts of unbound  $\beta$ -catenin, which translocate to the nucleus and induce expression of cell cycle genes.

The EGFR pathway is often implicated as an important mechanism in carcinogenesis of various organs, espe-

\*Hospital Feldkirch, Affiliation of the Medical University Innsbruck, Institute for Pathology, Carinagasse, Feldkirch; †Department of Internal Medicine, Division of Hematology and Oncology, Medical University Innsbruck, Anichstrasse, Innsbruck; ‡Department of Pneumology, Hospital Natters, In der Stille, Natters; §Institute for Clinical Epidemiology, ||Department of Visceral, Transplantation and Thoracic Surgery, Medical University Innsbruck, Innsbruck; ¶IIIrd Medical Department for Hematology, Oncology, Hemostasiology, Infectious Diseases and Rheumatology, University Hospital Salzburg, Müllner Hauptstrasse, Salzburg, Austria; and #Institute for Pathology, University Hospital Basel, Schoenbeinstrasse, Basel, Switzerland.

Disclosure: The authors declare that no funding was received for this work. Address for correspondence: W. Sterlacci, MD, Hospital Feldkirch, Affiliation of the Medical University Innsbruck, Institute for Pathology, Carinagasse 47, 6807 Feldkirch, Austria; and Medical University Innsbruck, Institute for Pathology, Muellerstrasse 44, 6020 Innsbruck, Austria. E-mail: william.sterlacci@lkhf.at

Copyright © 2010 by the International Association for the Study of Lung Cancer

ISSN: 1556-0864/10/0509-1325

cially in non-small cell lung cancer (NSCLC).<sup>5</sup> It is known to affect cancer cell proliferation, apoptosis, angiogenesis, and metastatic spread.<sup>5</sup> After ligand binding, an intracellular tyrosine kinase domain of EGFR is autophosphorylated, activating several downstream signaling pathways, including signal transducer and activator of transcription (STAT) and phosphatidylinositol-3' kinase (PI3K). Of the seven known members of the STAT family, especially STAT3 has been shown to be activated in many malignancies.<sup>6</sup> STATs have been described as playing an important role in hematologic neoplasms, and increasingly in solid cancers, such as those of prostate, pancreas, breast, and head and neck.<sup>7,8</sup> Activated STAT3 has also been implied as a marker of poor prognosis in some tumors.<sup>9</sup>

PI3K, which is recruited by activated growth receptor tyrosine kinases, such as EGFR, undergoes allosteric activation of its catalytic subunit and then phosphorylates phosphatidylinositol-4,5-bisphosphate (PIP2) on the intracellular plasma membrane, generating phosphatidylinositol-3,4,5-trisphosphate (PIP3). Then, Akt translocates and interacts with PIP3, resulting in tyrosine phosphorylation of Akt. Thereby activated Akt (pAkt) then phosphorylates several cellular proteins and may enter the nucleus, facilitating cell survival, cell growth, and cell cycle entry.<sup>10</sup> Among other events, the degradation of the cytoplasmic signaling molecule  $\beta$ -catenin is inhibited, which then translocates to the nucleus and combines with transcription factors, causing expression of genes such as *cyclin D1* (*CCND1*).<sup>11</sup> pAkt phosphorylates, p21, inhibit its antiproliferative effects as a cyclin-dependent kinase (CKD) inhibitor (CKI) by retaining it in the cytoplasm, which has also been described for p27, another CKI of the same family (kinase-inhibitory protein/CDK-inhibitory protein [KIP/CIP]).<sup>11</sup> In addition, pAkt has been identified as an independent prognostic factor associated with decreased survival.<sup>12</sup> Phosphatase and tensin homologue (PTEN) negatively regulates PI3K-induced signaling by converting PIP3 back to PIP2, thus acting as a tumor suppressor.

Merely part of the downstream signaling pathways of EGFR is described here, which already becomes very complex and intertwined (Figure 1). One can readily appreciate the difficulty in targeted pharmacologic therapies, considering the variety of evasion possibilities. It becomes clear that EGFR with its multiple downstream components involved in various signaling pathways plays a central role in tumorigenesis. The different mechanisms of deregulation, including gene mutations and amplifications, provide tumor cells with a constantly activated pathway. Most of the numerous existing reports involving EGFR pathways deal with a single, or few downstream molecules. A likely key to gain further insight here is to analyze a more extensive portion of the complex EGFR signaling mechanisms. To obtain significant correlations and improve biologic risk assessment, we considered EGFR-signaling related factors associated with EMT and with control over the G1 cell cycle-phase in NSCLC. The aim of this study was to establish markers (or marker panels) in routine

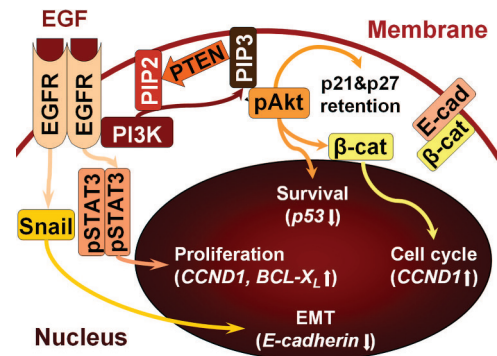


**FIGURE 1.** Signaling pathways of the epidermal growth factor receptor. EGFR, epidermal growth factor receptor; EMT, epithelial–mesenchymal transition; pAkt, phosphorylated Akt; PTEN, phosphatase and tensin homologue; pSTAT3, phosphorylated signal transducer and activator of transcription 3; PI3K, phosphatidylinositol-3' kinase;  $\beta$ -cat,  $\beta$ -catenin; E-cad, E-cadherin; PIP2, phosphatidylinositol-4,5-bisphosphate; PIP3, phosphatidylinositol-3,4,5-trisphosphate; EMT, epithelial–mesenchymal transition; *CCND1*, cyclin D1 gene.

histologic analysis, which might enable the pathologist a clinically relevant prognostic grouping.

## PATIENTS AND METHODS

### Patients

The archival samples derived from 405 lung cancer patients radically operated between 1992 and 2004 and diagnosed with NSCLC at the Institute for Pathology, Medical University of Innsbruck. Cases were selected only based on tissue preservation. Hematoxylin and eosin (H&E) stains from all available slides (complete tumor sample) of all cases were reclassified by two pathologists (W.S. and A.T.) without the knowledge of patient information, according to the current World Health Organization (WHO) classification of tumors of the lung as described previously.<sup>13,14</sup> Categories included squamous cell carcinoma (SCC), adenocarcinoma (ACA), large cell carcinoma (LCC), adenosquamous carcinoma, sarcomatoid carcinoma (which were all of the pleomorphic type), and mucoepidermoid carcinoma. Cases containing less than 10% spindle cells or giant cells were noted as such, but classified according to the major histologic component present, as required by the WHO.<sup>13</sup> All cases were examined immunohistochemically concerning neuroendocrine differentiation as previously described.<sup>14</sup> Thus, in addition to classic LCC, a group of LCC with neuroendocrine differentiation arised (LCNEC), according to the current requirements of the WHO.<sup>13</sup> Carcinoids were not included. Tumor differentiation was graded as well, moderate, or poor. The clinical information was documented within the Twelve Years Retrospective of Lung Cancer survey, a project aiming at analyzing various features of a large number of lung cancer patients. These patients mainly originated from the Austrian county of Tyrol and were all diagnosed and treated at the Medical University Hospital

of Innsbruck and associated hospitals. Approval for data acquisition and analysis was obtained from the Medical University of Innsbruck Ethics Committee (the local Institutional Review Board). The basic patients' characteristics including symptoms at presentation, smoking habits, comorbidities, and laboratory parameters, as well as the complete course of treatment modalities, including surgery and all lines of chemo- and radiotherapy, was documented.<sup>15</sup> Regarding therapy modalities, the patients were routinely discussed at the Medical University of Innsbruck Tumor Board, and a state of the art recommendation of the therapy adapted to the condition of the patient was given. Accordingly, there was a continuous shift of therapy modalities routinely applied in this comparably large interval of patients recruited to the survey.<sup>15,16</sup>

### Tissue Microarray Construction

Tumor material consisted of paraffin-embedded tissue after fixation in 10% neutral buffered formalin. The tissue microarray (TMA) was constructed as previously described.<sup>14</sup> Briefly, representative tumor areas were marked on H&E stained slides and four cylindrical 0.6-mm tissue cores each were arrayed from the corresponding paraffin blocks into a recipient block, using an arraying machine from Beecher Instruments. The core coordinates were recorded for exact location using Microsoft Excel and printouts assisted the subsequent immunohistochemical evaluation. Four-micrometer-thick paraffin sections were cut. The first sections were stained with H&E to confirm validity, and the other sections were used for immunohistochemistry. Adhesive transfer tape was not used.

### Immunohistochemistry

Immunohistochemistry was performed using the automated staining systems, Ventana Benchmark XT and Nexes received from Ventana Medical Systems Inc. (Tucson, AZ), except for pSTAT3, cyclin D2 and D3, cyclin E, p21 and p27 stainings, which were incubated overnight at 4°C and stained using the ABC method. The primary antibodies used and their dilutions are listed in Table 1.

### Immunohistochemical Evaluation

Only spots containing at least 20 vital tumor cells were evaluated. If all four spots of a case did not meet this criterion it was excluded. Tumor cells were counted independently by two pathologists (W.S. and A.T.) to study agreement between the observers and the percentage of positive cells, staining localization was also noted for each spot, followed by the calculation of the arithmetic mean value. The only exception was the evaluation of EGFR staining, which was scored according to the EGFR pharmDx Interpretation Manual by Dako (Glostrup, Denmark). EGFR-negative (0): absence of membrane staining above background in all tumor cells; EGFR-positive (staining intensity: 1+, 2+, or 3+): any staining of tumor cell membranes above background level, whether complete or incomplete circumferential staining.

### CCND1 Fluorescence In Situ Hybridization

The *CCND1* gene status was assessed independently by two pathologists (E.O. and A.T.) by fluorescence in situ

**TABLE 1.** Applied Antibody Panel

Antibody	Source	Dilution	Retrieval
EGFR	Ventana 790-2988	Prediluted	Protease 1 12'
pAkt	Abcam ab8932	1:450	Citrate pH 6, autoclave 120°C 5'
PTEN	Novocastra NCL-PTEN	1:200	CC1
Snail	Abgest AP2054a	1:50	ER2 pH 9, microwave 100°C 20'
β-Catenin	Ventana 760-4242	Prediluted	CC1
E-cadherin	DAKO IRO59	Prediluted	Citrate pH 6, microwave 80°C 30'
PI3K	BD Bioscience 610046	1:1000	ER2 pH 9, microwave 100°C 20'
pSTAT3	Cell Signaling 9145	1:50	TEC pH 9, microwave 100°C 30'
Cyclin D1	DCS CI677C01	1:50	Citrate pH 6, microwave 100°C 30'
Cyclin D2	Santa Cruz sc-181	1:8000	Citrate pH 6, microwave 98°C 60'
Cyclin D3	Novocastra NCL-Cyclin D3	1:80	Citrate pH 6, microwave 98°C 60'
Cyclin E	Neomarkers MS-1060-S	1:20	Citrate pH 6, microwave 98°C 60'
p27	Neomarkers MS-256	1:250	Citrate pH 6, microwave 98°C 60'
p21	Thermo MS-387-P	1:400	Citrate pH 6, microwave 98°C 60'

EGFR, epidermal growth factor receptor; pAkt, phosphorylated Akt; PTEN, phosphatase and tensin homologue; pSTAT3, phosphorylated signal transducer and activator of transcription 3; PI3K, phosphatidylinositol-3' kinase.

hybridization (FISH) using dual-color, break-apart probes (from Vysis/Abbott, Downers Grove, IL; *CCND1*: order no. 05J96-001) on paraffin-embedded tissue sections according to the protocol published by Vysis/Abbott ([www.abbottmolecular.com](http://www.abbottmolecular.com)). Slides were counterstained with 125 ng/ml of 4',6-diamino-2-phenylindole in antifade solution. FISH signals were scored with a Zeiss fluorescence microscope equipped with double-band pass filters for simultaneous visualization of Spectrum Green and Spectrum Orange signals. Cases on the TMA were considered evaluable for FISH if at least 200 tumor cell nuclei per core displayed positive signals. Splits were recorded as percentage of cells bearing an abnormality of all the analyzed cells. The cutoff score to consider a case rearranged was the mean plus 3SDs of split nuclei in the reference cases (i.e., 9%). The minimal distance of split signals was defined as at least three single-signal widths. High-level amplification was defined as presence of either more than 10 gene signals or tight clusters of at least five gene signals. Polysomies and low-level amplifications of *CCND1* (termed together "gains") were defined as presence of tumor cell nuclei with three or more signals exceeding the mean plus 3SDs of tri-/polysome nuclei in reference normal lung parenchyme (i.e., >10% tumor cells with >3 fused signals).

### EGFR Fluorescence In Situ Hybridization

The *EGFR* gene status was assessed independently by two pathologists (E.O. and A.T.) by FISH using dual-color

probes (LSI 7p12 EGFR spectrum orange and CEP7 7p11.1-q11.1 spectrum green from Vysis/Abbott; order no. 05J48-001) to the protocol published by Vysis/Abbott (www.abbottmolecular.com). Patients were classified into five FISH strata with ascending number of copies of the EGFR gene per cell according to Cappuzzo's criteria: (1) disome ( $\leq 2$  copies in  $>90\%$  of cells), (2) low-grade amplified ( $\leq 2$  copies in  $\geq 40\%$  of cells, three copies in  $\geq 10\%$  of the cells,  $\geq 4$  copies in  $<10\%$  of cells), (3) low polysome ( $\geq 4$  copies in 10–40% of cells), (4) high polysome ( $\geq 4$  copies in  $\geq 40\%$  of cells), and (5) amplified cases (defined by presence of tight *EGFR* gene clusters and a ratio of *EGFR* gene to chromosome of  $\geq 2$  or  $\geq 15$  copies of *EGFR* per cell in  $\geq 10\%$  of analyzed cells).<sup>17</sup>

### Statistical Analysis

The degree of agreement between observers was evaluated by interclass correlation coefficients, using reliability Cronbach's alpha analysis. Multivariable analysis of clinicopathological and immunohistochemical parameters was performed using the Spearman test corrected for multiple testing, considering *p* less than 0.0031 as significant. In addition, for the three major histology types (ACA, SCC, and LCC), the mean percentage of positively stained cells was compared, and significant markers (*p* [ANOVA]  $<0.005$ ) were further analyzed using the Kruskal-Wallis-H test. The prognostic relevance of respective markers was assessed by means of receiver operating characteristic analysis, selecting death as the state variable. Optimal cutoff values were calculated using the Youden index (J) for variables demonstrating an asymptomatic significance less than 0.2 and an adequately shaped receiver operating characteristic curve, otherwise the median was selected.<sup>18</sup> Kaplan-Meier curves were calculated for survival estimates, and a log-rank statistic was used to determine differences between groups. Survival estimates for dual combinations of markers were analyzed together as: either markers negative, any one marker positive, or both markers positive. All parameters with at least 10 deaths and a *p* less than 0.1 for overall survival estimates by the Kaplan-Meier method were analyzed by the multivariable Cox regression model. The value of *p* less than 0.05 was considered as significant. Two-sided tests were used throughout. Statistical calculations were performed using SPSS 17.0 software (SPSS, Chicago, IL).

## RESULTS

### Histopathology and Patient Characteristics

The tumor samples were derived from 405 radically operated patients. After revision of all 405 cases, 207 were diagnosed with ACA, 126 SCC, 58 LCC (including 16 LCNEC) nine adenosquamous carcinoma, four pleomorphic, and one mucoepidermoid carcinoma. Distribution of pathologic tumor stage by Union Internationale Contre le Cancer (UICC) revealed 196 stage I, 61 stage II, 54 stage IIIA, 19 stage IIIB, and 14 stage IV. For 61 patients, the definite tumor stage was not feasible. The patient population comprised 290 men and 115 women with an average age of 62 years and a range from 23 to 84 years (Table 2).

**TABLE 2.** Clinicopathological Characteristics

Characteristic	No. of Patients (N = 405)	%
Age (yr)		
Median (range)	62 (23–84)	
<64	218	53.8
>64	187	46.2
Gender		
Male	292	72.1
Female	113	27.9
pUICC stage		
I	203	50.1
II	61	15.1
IIIA	54	13.3
IIIB	19	4.7
IV	14	3.5
Unknown	54	13.3
Histology		
Adenocarcinoma	207	51.1
Squamous cell carcinoma	126	31.1
Large cell carcinoma	56	13.8
Others	16	4
Sarcomatoid component		
None	390	96.3
<10%	11	2.7
>10%	4	1
Differentiation		
Well	21	5.2
Moderate	170	42
Poor	214	52.8
T stage		
1	132	32.6
2	187	46.2
3	27	6.6
4	17	4.2
Unknown	42	10.4
N stage		
0	195	48.2
1	86	21.2
2	43	10.6
Unknown	81	20
Smoking status		
Never smoker	15	3.7
Smoker	181	44.7
Unknown	209	51.6

pUICC, pathological Union Internationale Contre le Cancer.

### Immunohistochemistry

Cronbach's alpha for interobserver reproducibility of the immunohistochemical markers was excellent (at least 0.87 for PTEN). Positive staining for cyclin D1, cyclin D2, cyclin D3, cyclin E, p21, pSTAT3, Snail, and PTEN was observed exclusively nuclear (Figure 2A–E, H, N, P). Along with an unequivocal nuclear signal, pAkt demonstrated additional cytoplasmic staining in some cases, which was extremely faint and not taken into account for further analysis

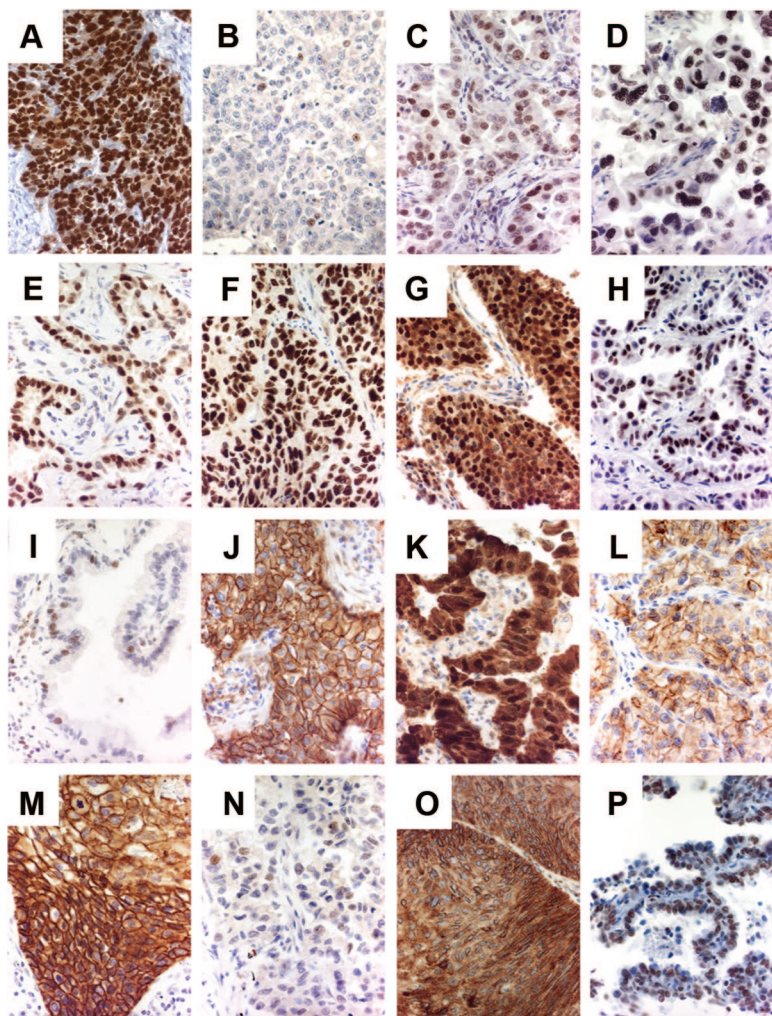


**FIGURE 2.** Immunohistochemical expression of cyclin D1 (A), cyclin D2 (B), cyclin D3 (C), cyclin E (D), p21 (E), nuclear p27 (F), cytoplasmic p27 (G), phosphorylated signal transducer and activator of transcription 3 (H), phosphorylated Akt (I), membranous  $\beta$ -catenin (J), nuclear  $\beta$ -catenin (K), E-cadherin (L), epidermal growth factor receptor (M), Snail (N), phosphatidylinositol-3' kinase (O), and phosphatase and tensin homologue (P) in non-small cell lung cancer tissue microarray samples. Original magnification  $\times 400$ .

(Figure 2I). EGFR demonstrated a complete or incomplete membranous pattern, along with a fainter-stained cytoplasm (Figure 2M). E-cadherin demonstrated a mostly incomplete membranous pattern with a fainter-stained cytoplasm and PI3K stained the cytoplasm with a membranous accentuation (Figure 2L, O). The staining localization for p27 was observed in the nucleus as well as in the cytoplasm, often concomitant (Figure 2F, G). Both patterns were recorded separately. Considering  $\beta$ -catenin, two staining patterns were also observed: a membranous and a nuclear signal (Figure 2J, K). Because the membranous  $\beta$ -catenin staining pattern was absent only in a single case, it was excluded from further analysis. Quantitative immunohistochemical data are shown in Table 3.

### FISH Analysis

EGFR FISH was successful in 210 cases, whereas *CCND1* FISH succeeded only in 160 cases. Cronbach's alpha for interobserver reproducibility of FISH analyses was excellent (0.95 for EGFR and 0.98 for *CCND1*). The respective EGFR status is shown in Table 4 and Figure 3A. Twelve of 54 SCC, nine of 76 ACA, and six of 26 LCC (including 3/5 LCNEC) showed high-level amplifications of the *CCND1*

gene, whereas nine of the 54, 19 of the 76, and three of the 26 (1/5 LCNEC) showed low-level gains, respectively (Figure 3B). Two cases, one SCC and one LCC each, showed split red and green signals corresponding to *CCND1* gene rearrangements; in the case of SCC, the number of free red (telomeric) signals significantly exceeding that of the green (centromeric) ones, suggesting an unbalanced translocation with double minutes (Figure 3C). A "gene dosage effect" was highly likely, because cases ( $n=100$ ) without numeric alterations of the *CCND1* gene expressed cyclin D1 in a mean of  $7.5 \pm 12.4\%$  of cells, whereas cases with low-level gains ( $n = 31$ ) expressed cyclin D1 in  $15.5 \pm 19.4\%$  and those with high-level amplifications ( $n = 28$ ) expressed cyclin D1 in  $31.6 \pm 23.7\%$  of tumor cells ( $p < 0.001$ ). Immunohistochemical expression of EGFR protein increased with increasing gene copy number by FISH ( $\rho = 0.255$ ) and cyclin D1 expression correlated with *CCND1* gene copy number by FISH ( $\rho = 0.477$ ).

### Correlations Between Variables

The results of the correlation analysis are demonstrated in Tables 5 and 6. The strongest correlation was found between cytoplasmic and nuclear expression of p27. Import-

**TABLE 3.** Immunohistochemical Expression Profiles

Parameter	Evaluable Cases	Percentage of Stained Cells				Cases Above Cutoff (%)
		Median	Mean	Range	Cutoff	
p27 Nuclear	382	20	30.2	0–100	45	111 (29.1)
p27 Cytoplasmic	381	20	33.4	0–100	20	225 (59.1)
p21	383	16.7	23.9	0–95	16	194 (50.7)
Cyclin D1	390	5	11.9	0–100	15	100 (25.6)
Cyclin D2	265	0	4.3	0–70	0	109 (41.1)
Cyclin D3	391	2	7.5	0–90	3.5	167 (42.7)
Cyclin E	389	0.66	6.1	0–80	0.66	193 (49.6)
PI3K	382	100	97.1	30–100	100	290 (75.9)
PTEN	379	0	8.4	0–100	0	57 (15)
pAkt	366	0	5.6	0–80	0	152 (41.5)
$\beta$ -Catenin nuclear	391	0	0.95	0–80	0	10 (2.6)
E-cadherin	391	20	34.1	0–90	25	190 (48.6)
pSTAT3	384	0	1.3	0–36.6	0	56 (14.6)
Snail	376	0	0.27	0–10	0	27 (7.2)
EGFR	383	Score 0: 198 2+: 69		1+: 60 3+: 56	0	185 (48.3)

PI3K, phosphatidylinositol-3' kinase; PTEN, Phosphatase and tensin homologue; pAkt, phosphorylated-Akt; pSTAT3, phosphorylated signal transducer and activator of transcription 3; EGFR, epidermal growth factor receptor.

**TABLE 4.** EGFR FISH Analysis According to Histological Lung Cancer Type

FISH Status	Total (N = 210)	ACA	SCC	LCC	PLM	ASC	MEC
Disome/diploid	53 (25.2)	26 (30.6)	17 (21.5)	10 (27.1)	0	0	0
Low-grade amplified	14 (6.7)	8 (9.4)	4 (5.1)	1 (2.7)	0	1 (16.7)	0
Amplified	16 (7.6)	4 (4.7)	11 (13.9)	0	0	1 (16.7)	0
Low polysomy/polyploidy	115 (54.8)	43 (50.6)	39 (49.4)	26 (70.2)	2 (100)	4 (66.6)	1 (100)
High polysomy/polyploidy	12 (5.7)	4 (4.7)	8 (10.1)	0	0	0	0

Data are expressed as N (%).

EGFR, epidermal growth factor receptor; FISH, fluorescence in situ hybridization; ACA, adenocarcinoma; SCC, squamous cell carcinoma; LCC, large cell carcinoma; PLM, pleomorphic carcinoma; ASC, adenosquamous carcinoma; MEC, mucocypidermoid carcinoma.

tantly, cyclins (D1, D2, D3, and E) were associated with CKIs (p21 and p27). Furthermore, EGFR gains and overexpression were determined by FISH and immunohistochemistry, respectively, significantly cohered to SCC when compared with other histologic types ( $p = 0.004$  and  $p < 0.001$ , respectively). Accordingly, ACA demonstrated a negative correlation with EGFR expression ( $p = 0.001$ ). T and N stage did not show significant correlations with the examined biomarkers.

### Survival Analysis

All results for calculations of survival estimates are shown in Table 7. Male gender, age  $>64$  years, pUICC  $> I$ , T stage  $>1$ , N stage  $>0$ , and sarcomatoid carcinoma were associated with a significantly worse overall survival time, as well as patients expressing E-cadherin, nuclear p27, or cyclin D3 above respective cutoff levels (Figure 4A–C). Cyclin D1 was not a significant parameter by univariable analysis (Figure 4D). When EGFR immunohistochemistry results were categorized as either positive

(scores  $\geq 1$ ) or negative (score = 0), a significantly decreased overall survival time was noted for EGFR positive cases (Figure 4E). When analyzed stratified according to the major histologic subtypes, SCC, ACA and LCC, all subgroups still demonstrated a worse overall survival time when the above-mentioned markers were positive, although statistical significance was only achieved for the group of ACA (nuclear p27:  $p = 0.047$ , E-cadherin:  $p = 0.017$ , EGFR expression:  $p = 0.04$ ). When stratified with respect to pUICC stages I and  $> I$ ,  $p$  values did not reach statistical significance. A further reduction in overall survival time was noted for dual combinations of any of the markers EGFR, cyclin D1, cyclin D3, nuclear p27, and E-cadherin (all  $p \leq 0.03$ ) (Figure 4F). All the combinations again only achieved statistical significance in the group of ACA, when analyzed stratified according to the major histologic subtype. When analyzed according to stage, the combination of E-cadherin and EGFR expression was associated with a significantly reduced overall

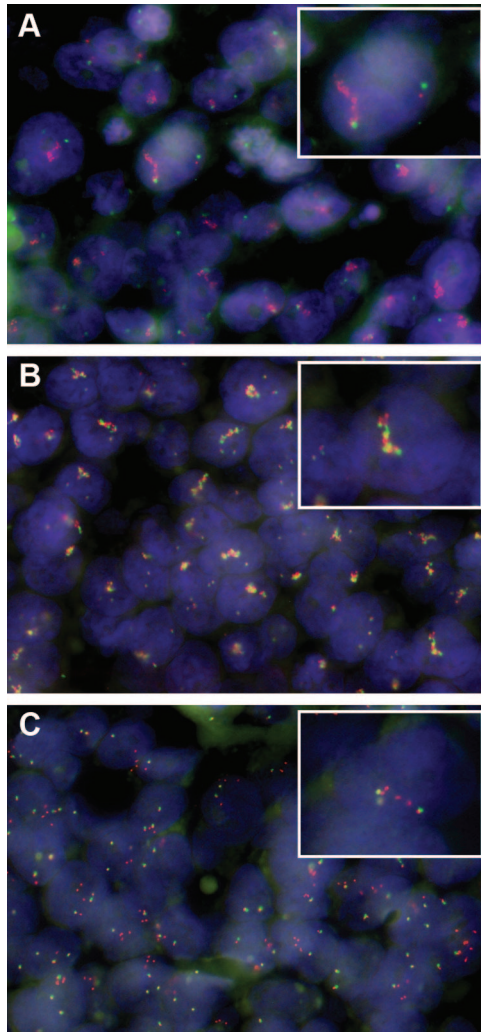


**FIGURE 3.** Fluorescence in situ hybridization analysis for epidermal growth factor receptor (*EGFR*) (A) and *Cyclin D1* (*CCND1*) genes (B, C). (A) Note highly increased numbers of red (*EGFR*) compared with green signals (centromere 7) corresponding to high-level amplification. (B) Note increased, but balanced red (telomeric) and green (centromeric) signals in tumor cells, due to amplification of doubled-colored probes flanking *CCND1*, corresponding to high amplification of *CCND1*. (C) Note split red (telomeric) and green signals (centromeric) as well as increased red signals corresponding to unbalanced translocation involving the *CCND1* locus on chromosome 11 with double minutes of the telomeric parts of the chromosome.

survival time for pUICC stage > I ( $p = 0.035$ ). Of all immunohistochemical parameters examined by multivariable analysis, cyclin D1 was identified as the only independent tumor-related marker indicating poor overall survival time (Table 8). When stratified according to major histologic subtype, multivariable analysis revealed cyclin D1 as the only significant marker indicating worse survival for SCC (relative risk: 2.912, 95% confidence interval [CI]: 1.399–6.064,  $p = 0.004$ ) and respectively age for LCC (relative risk: 3.779, 95% CI: 1.484–9.621,  $p =$

**TABLE 5.** Correlations Between Clinicopathological and Immunohistochemical Parameters

	pSTAT3	PTEN	Grade	Smoker	p27 Cytoplasmic	EGFR (IHC)	Cyclin D1	Cyclin E	PI3K	Cyclin D2	p21	p27 Nuclear
PI3K	0.001 (0.166)											
$\beta$ -Catenin nuclear	0.001 (0.170)											
pAkt	<0.001 (0.219)											
Cyclin E	<0.001 (0.301)											
pSTAT3	<0.001 (–0.194)	<0.001 (–0.346)										
E-cadherin	0.003 (–0.151)											
p21					<0.001 (0.178)	0.002 (0.163)	<0.001 (0.338)	<0.001 (0.313)				
PTEN	<0.001 (0.305)							0.003 (0.153)				
p27 Cytoplasmic	<0.001 (0.204)							<0.001 (0.215)	0.001 (–0.201)			
p27 Nuclear	<0.001 (0.262)	<0.001 (0.209)			<0.001 (0.514)		<0.001 (0.273)	<0.001 (0.229)	<0.001 (0.243)	<0.001 (–0.223)	0.001 (0.178)	
Cyclin D3	<0.001 (0.212)	<0.001 (0.237)			<0.001 (0.203)		<0.001 (0.302)	<0.001 (0.194)	<0.001 (0.194)		<0.001 (0.266)	<0.001 (0.466)

Data are given as  $p$  (spearman correlation coefficient).  
 PI3K, phosphatidylinositol-3' kinase; PTEN, phosphatase and tensin homologue; pAkt, phosphorylated-Akt; pSTAT3, phosphorylated signal transducer and activator of transcription 3; EGFR, epidermal growth factor receptor; IHC, immunohistochemistry.

**TABLE 6.** Correlations Between Immunohistochemical Parameters and Histological Tumor Type

Parameter	Mean Percentage of Stained Cells (SD)			<i>p</i> (Kruskal-Wallis-H)
	Adenocarcinoma	Squamous Cell Carcinoma	Large Cell Carcinoma	
pSTAT3	1.9 (5.4)	0.5 (2.9)	0.4 (1.9)	<0.001
Nuclear p27	33.7 (29.1)	22.3 (22.9)	38.4 (24.7)	<0.001
Cytoplasmic p27	42.6 (33.8)	19.7 (21.3)	34.3 (29.6)	<0.001
p21	20.4 (21.5)	32.1 (22.8)	20.1 (21.5)	<0.001
E-cadherin	43.9 (32.9)	21.5 (25.4)	26.8 (29.9)	<0.001
Cyclin D1	11.8 (17.7)	11.8 (16.6)	13.2 (19.5)	0.862
EGFR (IHC)	0.7 (1.1) <sup>a</sup>	1.4 (1.2) <sup>a</sup>	0.6 (0.9) <sup>a</sup>	<0.001

<sup>a</sup> Results indicate mean score (SD).

pSTAT3, phosphorylated signal transducer and activator of transcription 3; EGFR, epidermal growth factor receptor; IHC, immunohistochemistry.

0.005). For ACA, N stage (relative risk: 9.501, 95% CI: 2.695–33.488,  $p < 0.001$ ), pUICC (relative risk: 0.246, 95% CI: 0.7–0.863,  $p = 0.029$ ), T stage (relative risk: 1.729, 95% CI: 1.045–2.862,  $p = 0.033$ ), and cyclin D3 (relative risk: 1.729, 95% CI: 1.040–7.824,  $p = 0.035$ ) were significantly associated with decreased overall survival. Markers implicated in the process of EMT such as  $\beta$ -catenin and Snail clearly played a subordinate role. The impact of E-cadherin also became inferior when analyzed by multivariable testing.

## DISCUSSION

This study analyzes a large and intertwined group of interacting molecular factors, involving EGFR signaling, EMT, and G1 mitotic phase, which play an important role in cancerogenesis and progression of NSCLC. Numerous reports involving a single or only a few of the mentioned molecular markers exist, but success concerning potential correlations, structural and numeric gene aberrations of the respective genes and biologic risk assessment is still lacking. It has been stated that analysis of multiple markers is most likely superior to any single marker for the prediction of clinical outcome in NSCLC.<sup>19</sup> A reasonable and comprehensible approach is to investigate the impact of different factors known to be involved with one and another. In addition to a multitude of interlinked molecular factors, this study has the advantage of a large patient group with extensive clinical data available, and a follow-up period of up to 14.5 years after surgical tumor resection (median overall postoperative survival: 3.2 years). By applying a standardized TMA platform, an ideal method of evaluation was provided.<sup>20</sup>

Expressions of nuclear p27, cyclin D1, cyclin D3, E-cadherin, and EGFR were all identified as having a significant impact on overall survival time in NSCLC in curatively operated patients. Increased positive staining results for these factors were associated with a significant reduction in overall survival time. Reduced overall survival time was still obvious when the patient cohort was stratified according to histologic tumor subtype, but always only statistically significant for the group of ACA.

Among the CKIs, p27 regulates transition of the cell cycle from the G1 to the S phase by its activity as a potent inhibitor of cyclins complexed with CDK.<sup>21</sup> Because p27 must be localized to the nucleus to function as a CKI, mechanisms resulting in proteosomal degradation, nuclear export, or cytoplasmic retention will limit its activity and promote G1-S progression. Nuclear and cytoplasmic staining of p27 demonstrated a strong correlation with each other in this study, indicating a deregulation of p27, appreciable by its cytoplasmic localization. Reduced levels of p27 are frequent in human breast and colon cancers and have been associated with poor prognosis,<sup>22–24</sup> which has also been reported for NSCLC.<sup>25</sup> On the other hand, especially studies involving lymphomas have demonstrated that highly malignant neoplasias may also be associated with increased nuclear staining of p27.<sup>26,27</sup> An explanation for this somewhat controversial finding is the association with increased expression of cyclins, causing nuclear sequestration of p27.<sup>26</sup> This suggests that p27 protein in these cases is rendered nonfunctional as an inhibitor of cell-cycle progression. Indeed, our results also demonstrate a significant correlation between increasing nuclear p27 expression and increased cyclin D1, cyclin D3, and cyclin E. In addition, these cyclins were also significantly associated with increased expression of p21, another CKI of the same molecular family (CIP/KIP) as p27. Our results emphasize that the interpretation of immunohistochemical staining of p27 is not always straight forward. An increased nuclear staining result is not proof of normally functioning p27, but may indicate an abnormal sequestration of p27 protein. A similar scenario is often described for p16 in cervical squamous carcinoma.<sup>28</sup> p16, a CKI of the INK4/ARF family, whose overexpression has repeatedly been reported to be typical of dysplastic and neoplastic epithelium of the cervix, slows down the cell cycle by inactivating the CDK that phosphorylates the tumor suppressor retinoblastoma protein (pRb).<sup>29</sup> In analogy, p16 overexpression in cervical lesions is hypothesized to be caused by the functional inactivation of Rb.<sup>30</sup>

Loss of E-cadherin has often been reported in association with tumor progression<sup>31–33</sup> and poor prognosis.<sup>34</sup> Our results show a reduction in E-cadherin expression in every



**TABLE 7.** Postoperative Overall Survival Analysis by Kaplan-Meier Estimates According to Clinicopathological and Immunohistochemical Parameters

Variables	No. of Patients	Median Postoperative OS (mo)	<i>p</i>
Gender			
Male	292	37.8	<b>0.012</b>
Female	113	74.8	
Age			
<64	218	66.8	<b>0.003</b>
>64	187	37.8	
Histology			
Adenocarcinoma	207	45.4	0.361
Squamous cell carcinoma	126	49.6	
Large cell carcinoma	58	31.5	
Sarcomatoid			
<10%	401	45	<b>&lt;0.001</b>
≥10%	4	9.1	
T stage			
T1	132	74.8	<b>0.02</b>
T2–4	231	40.1	
N stage			
N0	195	83.8	<b>&lt;0.001</b>
N1–2	129	28.3	
pUICC			
I	203	75.9	<b>&lt;0.001</b>
II–IV	148	31	
Smoker status			
Never smoker	15	65	0.941
Smoker	181	46.5	
p27 Nuclear			
Below cutoff	271	46.6	<b>0.019</b>
Above cutoff	111	35	
p27 Cytoplasmic			
Below cutoff	156	42.1	0.58
Above cutoff	225	45	
p21			
Below cutoff	189	40.7	0.537
Above cutoff	194	47.7	
Cyclin D1 (IHC)			
Below cutoff	290	47.4	0.07
Above cutoff	100	39.1	
Cyclin D2			
Below cutoff	156	43.8	0.725
Above cutoff	109	41.7	
Cyclin D3			
Below cutoff	224	47.7	<b>0.019</b>
Above cutoff	167	44	
Cyclin E			
Below cutoff	196	45.4	0.442
Above cutoff	193	44.7	
Cyclin D1 (FISH)			
Negative	132	44	0.536
High-level gains	19	35	

Variables	No. of Patients	Median Postoperative OS (mo)	<i>p</i>
PI3K			
Below cutoff	92	36.8	0.307
Above cutoff	290	46.4	
PTEN			
Below cutoff	322	44.5	0.787
Above cutoff	57	46.5	
pAkt			
Below cutoff	214	45.4	0.598
Above cutoff	152	42.9	
EGFR (IHC)			
Negative	198	58.9	<b>0.027</b>
Positive	185	36.2	
EGFR (FISH)			
Negative	182	47.6	0.205
High polysomy or amplification	28	36.8	
Beta-catenin nuclear			
Below cutoff	381	45.4	0.232
Above cutoff	10	15.4	
E-cadherin			
Below cutoff	201	59.5	<b>0.026</b>
Above cutoff	190	36.2	
pSTAT3			
Below cutoff	328	44.7	0.776
Above cutoff	56	48.2	
Snail			
Below cutoff	349	45	0.552
Above cutoff	27	82.4	

PI3K, phosphatidylinositol-3' kinase; PTEN, phosphatase and tensin homologue; pAkt, phosphorylated-Akt; pSTAT3, phosphorylated signal transducer and activator of transcription 3; EGFR, epidermal growth factor receptor; IHC, immunohistochemistry; FISH, fluorescence in situ hybridization; pUICC, pathological Union Internationale Contre le Cancer.

Bold text indicates statistically significant *P* values.

evaluable NSCLC case. Nearly half (45.5%) the cases contained only up to 10% positively stained tumor cells, and not in a single case stained more than 90% of the tumor cells. Other reports have even considered more than 90% of stained tumor cells as the cutoff level for a positive E-cadherin status.<sup>35</sup> Loss of E-cadherin correlated with loss of differentiation in our study, a finding well in line with other reports.<sup>36</sup> After establishing a prognostically relevant cutoff level, our series demonstrated a significantly reduced overall survival time for patients with E-cadherin positive tumors. For a reliable interpretation of this finding, the staining pattern plays an important role. Analysis of the staining results revealed a mostly incomplete membranous pattern of the tumor cells with additional invariable staining of the cytoplasm. This is in contrast to the expected complete, exclusively membranous pattern in normal tissue.<sup>35</sup> Cytoplasmic localization of E-cadherin has been attributed to loss of normally functioning membranous E-cadherin with subsequent cytoplasmic accumulation.<sup>32</sup> This underlines the importance of precise analysis of staining results for accurate interpretation. In our series, all cases demonstrated a reduced level of E-cadherin expression and an abnormal staining

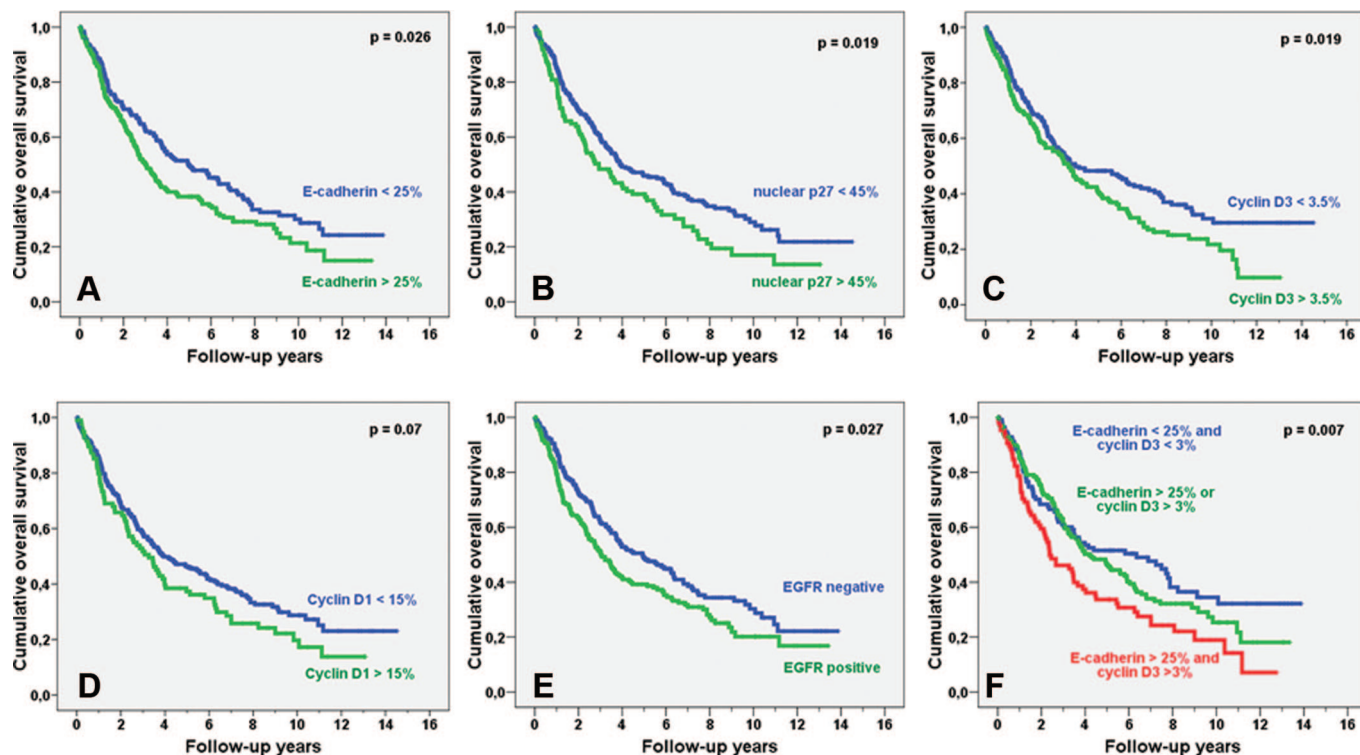


FIGURE 4. Kaplan-Meier survival estimate graphs comparing cases above and below cutoff levels for E-cadherin (A), nuclear p27 (B), cyclin D3 (C), cyclin D1 (D), EGFR (E), and combination of E-cadherin and cyclin D3 (F).

TABLE 8. Multivariable Cox Proportional Hazard Analysis of Overall Survival

Parameter	Relative Risk	95% CI	<i>p</i>
N stage (N0 vs. >N0)	3.521	1.917–6.469	<b>&lt;0.001</b>
Age, yr (<64 vs. >64)	1.770	1.275–2.458	<b>0.001</b>
Cyclin D1 (below vs. above cut-off)	1.577	1.090–2.282	<b>0.016</b>
Female vs. male	1.420	0.980–2.58	0.064
pUICC stage (I vs. >I)	0.625	0.344–1.142	0.127
E-cadherin (below vs. above cut-off)	1.208	0.878–1.662	0.245
T-stage (T1 vs. >T1)	1.229	0.865–1.747	0.250
EGFR (IHC) (score 0 vs. >0)	1.197	0.864–1.657	0.279
Cyclin D3 (below vs. above cut-off)	1.153	0.810–1.642	0.430
p27 nuclear (below vs. above cut-off)	1.064	0.715–1.583	0.761

EGFR, epidermal growth factor receptor; IHC, immunohistochemistry; pUICC, pathological Union Internationale Contre le Cancer.

Bold text indicates statistically significant *P* values.

pattern, indicating a deregulation of E-cadherin. Therefore, tumors above the calculated cutoff value in our cohort (higher percentage of abnormally stained cells) most likely represent tumors with a more advanced stage in deregulation of E-cadherin.

EGFR expressing cases were associated with a significantly decreased overall survival time when compared with EGFR negative cases, which has been widely reported.<sup>37</sup> Significantly increased *EGFR* gene copy number (amplification or high polysomy/-ploidy) was accompanied by worse

overall survival time, although without reaching statistical significance. A positive correlation between EGFR expression and *EGFR* FISH status was obvious. This supports previous reports stating that overexpression of EGFR by immunohistochemistry is associated with increased *EGFR* gene copy numbers by FISH analysis.<sup>38</sup> Also in line with most other studies is the association between EGFR expression and SCC, although contradictory results have been reported.<sup>39</sup> Interestingly, cases positive for any dual combination of the immunohistochemical markers, nuclear p27, cyclin D1, or cyclin D3 with EGFR, were all associated with a further decrease in overall survival time.

At multivariable analysis, cyclin D1 was identified as the only independent marker indicating poor overall survival time in our cohort. Although reports concerning cyclin D1 in NSCLC offer divergent conclusions, our finding is well in line with most others, especially recently published studies.<sup>40</sup> Cyclin D1 is often both amplified and overexpressed in NSCLC and preinvasive bronchial lesions. Marchetti et al.<sup>41</sup> found that 32% of their lung cancer cohort (N = 57) demonstrated increased gene copy numbers of *CCND1* and 44% were positive immunohistochemically. Betticher et al.<sup>42</sup> reported similar results (15% and 47%, respectively, N = 53). The discrepancy can be explained by the amount of gene copies that were required for considering *CCND1* as amplified (twofold for the former and threefold for the latter group). The results of our comparably large series support and considerably extend these findings, because altogether more than 35% of

NSCLC cases showed *CCND1* gains (17.5% high-level and 19.4% low-level gene amplifications, N = 160). In addition, the coincidence between *CCND1* gene amplification and increased cyclin D1 protein expression was obvious, which has been found in NSCLC and other tumors.<sup>43,44</sup> Importantly, cyclin D1 expression has been associated with EGFR-mutant lung cancer cells, which proved to be sensitive to the cyclin-dependent kinase inhibitor flavopiridol, confirming the functional relevance of the cyclin D axis.<sup>45</sup> Our data did not show significant correlations between EGFR and cyclin D1, concerning either gene levels or protein expression.

Our study puts special emphasis on the procedure of EMT, related to EGFR signaling, by integrating a number of molecules currently considered as playing an important role herein. Other than poor survival associated with aberrant expression of E-cadherin, we could not demonstrate any significant findings in this context. Sarcomatoid carcinomas did show a significant reduction in overall survival time compared with other histologic subtypes, but the former group consisted of only four cases. In addition, while two cases were in stage IB, the other two were in an advanced stage (IIIA and IV). This small number of sarcomatoid carcinomas does not allow meaningful conclusions; also, the advanced stage in half these cases is the most likely explanation for the dismal outcome. It must be stressed that although sarcomatoid carcinomas are likely due to EMT, this is not essentially necessary. For further support, molecular factors implicated in EMT were taken into account, which largely proved irrelevant for prognosis.

In conclusion, our study demonstrates the important impact that deregulation of p27, cyclin D1, and D3 has for the prognosis of NSCLC patients, indicating significantly decreased overall survival time. Especially, cyclin D1 proved to be a valuable marker, being the only (of multiple) independent molecular tumor-related factor with prognostic significance. Age was proved to be an independent parameter with prognostic significance indicating decreased overall survival by multivariable analysis. In contrast, the gender associated survival difference was still obvious, but not significant by multivariable analysis. When stratified according to age (<64 versus >64 years), survival analysis showed the same tendency as described for the entire cohort. Notably, the only parameter here associated with a lower *p* value in the subgroup analysis was nuclear p27 expression for patients younger than 64 years (*p* = 0.008). Analogous to the *EGFR* gene, the recurrent numeric aberrations of the *CCND1* gene in NSCLC, especially in SCC and LCC, including LCNEC emphasize its oncogenic relevance, which might also represent a potential treatment target in NSCLC. In operated patients, staining for cyclin D1 might be a reasonable additional analysis in routine diagnostics due to its prognostic information. It will have to be established whether this also holds true for NSCLC patients diagnosed in an advanced, nonoperable stage. Even more importantly, the value of prognostic markers should be tested both prospec-

tively and for their predictive value in terms of therapy efficacy.

## REFERENCES

- Lo HW, Hsu SC, Xia W, et al. Epidermal growth factor receptor cooperates with signal transducer and activator of transcription 3 to induce epithelial-mesenchymal transition in cancer cells via up-regulation of TWIST gene expression. *Cancer Res* 2007;67:9066–9076.
- Lu Z, Ghosh S, Wang Z, et al. Downregulation of caveolin-1 function by EGF leads to the loss of E-cadherin, increased transcriptional activity of beta-catenin, and enhanced tumor cell invasion. *Cancer Cell* 2003;4:499–515.
- Cano A, Pérez-Moreno MA, Rodrigo I, et al. The transcription factor snail controls epithelial-mesenchymal transitions by repressing E-cadherin expression. *Nat Cell Biol* 2000;2:76–83.
- Lee MY, Chou CY, Tang MJ, et al. Epithelial-mesenchymal transition in cervical cancer: correlation with tumor progression, epidermal growth factor receptor overexpression, and snail up-regulation. *Clin Cancer Res* 2008;14:4743–4750.
- Hynes NE, Lane HA. ERBB receptors and cancer: the complexity of targeted inhibitors. *Nat Rev Cancer* 2005;5:341–354; erratum 580.
- Bowman T, Garcia R, Turkson J, et al. STATs in oncogenesis. *Oncogene* 2000;19:2474–2488.
- Meier C, Hoeller S, Bourgau C, et al. Recurrent numeric aberrations of JAK2 and deregulation of the JAK2-STAT cascade in lymphomas. *Mod Pathol* 2009;22:476–487.
- Yu H, Jove R. The STATs of cancer—new molecular targets come of age. *Nat Rev Cancer* 2004;4:97–105.
- Kusaba T, Nakayama T, Yamazumi K, et al. Activation of STAT3 is a marker of poor prognosis in human colorectal cancer. *Oncol Rep* 2006;15:1445–1451.
- Engelman JA. The role of phosphoinositide 3-kinase pathway inhibitors in the treatment of lung cancer. *Clin Cancer Res* 2007;13:4637–4640.
- Fresno Vara JA, Casado E, de Castro J, et al. PI3K/Akt signalling pathway and cancer. *Cancer Treat Rev* 2004;30:193–204.
- David O, Jett J, LeBeau H, et al. Phospho-Akt overexpression in non-small cell lung cancer confers significant stage-independent survival disadvantage. *Clin Cancer Res* 2004;10:6865–6871.
- Travis W, Brambilla E, Müller-Hermelink H, et al. Pathology and Genetics of Tumours of the Lung, Pleura, Thymus and Heart. Lyon: IARC Press, 2004.
- Sterlacci W, Fiegl M, Hilbe W, et al. Clinical relevance of neuroendocrine differentiation in non-small cell lung cancer assessed by immunohistochemistry: a retrospective study on 405 surgically resected cases. *Virchows Arch* 2009;455:125–132.
- Fiegl M, Hilbe W, Auberger J, et al. Twelve-year retrospective analysis of lung cancer—the TYROL Study: daily routine in 1,424 patients (1995–2006). *J Clin Oncol* 2008;20:19063.
- Hilbe W, Aigner K, Dittrich C, et al. Expert recommendations 2006 on the rationale for second-line therapy for non-small cell bronchial neoplasms. *Wien Klin Wochenschr* 2007;119:259–266.
- Cappuzzo F, Hirsch FR, Rossi E, et al. Epidermal growth factor receptor gene and protein and gefitinib sensitivity in non-small-cell lung cancer. *J Natl Cancer Inst* 2005;97:643–655.
- Tzankov A, Zlobec I, Went P, et al. Prognostic immunophenotypic biomarker studies in diffuse large B cell lymphoma with special emphasis on rational determination of cut-off scores. *Leuk Lymphoma* 2010; 51:199–212.
- Yoo J, Jung JH, Lee MA, et al. Immunohistochemical analysis of non-small cell lung cancer: correlation with clinical parameters and prognosis. *J Korean Med Sci* 2007;22:318–325.
- Tzankov A, Went P, Zimpfer A, et al. Tissue microarray technology: principles, pitfalls and perspectives—lessons learned from hematological malignancies. *Exp Gerontol* 2005;40:737–744.
- Sherr CJ, Roberts JM. CDK inhibitors: positive and negative regulators of G1-phase progression. *Genes Dev* 1999;13:1501–1512.
- Loda M, Cukor B, Tam SW, et al. Increased proteasome-dependent degradation of the cyclin-dependent kinase inhibitor p27 in aggressive colorectal carcinomas. *Nat Med* 1997;3:231–234.
- Catzavelos C, Bhattacharya N, Ung YC, et al. Decreased levels of the

- cell-cycle inhibitor p27Kip1 protein: prognostic implications in primary breast cancer. *Nat Med* 1997;3:227–230.
24. Lloyd RV, Erickson LA, Jin L, et al. p27kip1: a multifunctional cyclin-dependent kinase inhibitor with prognostic significance in human cancers. *Am J Pathol* 1999;154:313–323.
  25. Singhal S, Vachani A, Antin-Ozerkis D, et al. Prognostic implications of cell cycle, apoptosis, and angiogenesis biomarkers in non-small cell lung cancer: a review. *Clin Cancer Res* 2005;11:3974–3986.
  26. Qi CF, Xiang S, Shin MS, et al. Expression of the cyclin-dependent kinase inhibitor p27 and its deregulation in mouse B cell lymphomas. *Leuk Res* 2006;30:153–163.
  27. Sánchez-Beato M, Camacho FI, Martínez-Montero JC, et al. Anomalous high p27/KIP1 expression in a subset of aggressive B-cell lymphomas is associated with cyclin D3 overexpression. p27/KIP1-cyclin D3 colocalization in tumor cells. *Blood* 1999;94:765–772.
  28. Ishikawa M, Fujii T, Masumoto N, et al. Correlation of p16INK4A overexpression with human papillomavirus infection in cervical adenocarcinomas. *Int J Gynecol Pathol* 2003;22:378–385.
  29. Volgareva G, Zavalishina L, Andreeva Y, et al. Protein p16 as a marker of dysplastic and neoplastic alterations in cervical epithelial cells. *BMC Cancer* 2004;4:58.
  30. Yildiz IZ, Usubütün A, Firat P, et al. Efficiency of immunohistochemical p16 expression and HPV typing in cervical squamous intraepithelial lesion grading and review of the p16 literature. *Pathol Res Pract* 2007;203:445–449.
  31. Lipponen P, Saarelainen E, Ji H, et al. Expression of E-cadherin (E-CD) as related to other prognostic factors and survival in breast cancer. *J Pathol* 1994;174:101–109.
  32. Elzagheid A, Kuopio T, Ilmen M, et al. Prognostication of invasive ductal breast cancer by quantification of E-cadherin immunostaining: the methodology and clinical relevance. *Histopathology* 2002;41:127–133.
  33. Kowalski PJ, Rubin MA, Kleer CG. E-cadherin expression in primary carcinomas of the breast and its distant metastases. *Breast Cancer Res* 2003;5:R217–R222.
  34. Liu LK, Jiang XY, Zhou XX, et al. Upregulation of vimentin and aberrant expression of E-cadherin/beta-catenin complex in oral squamous cell carcinomas: correlation with the clinicopathological features and patient outcome. *Mod Pathol* 2010;23:213–224.
  35. Lazř D, Tban S, Ardeleanu C, et al. The immunohistochemical expression of E-cadherin in gastric cancer: correlations with clinicopathological factors and patients' survival. *Rom J Morphol Embryol* 2008;49:459–467.
  36. Xu HT, Li QC, Zhang YX, et al. Connexin 43 recruits E-cadherin expression and inhibits the malignant behaviour of lung cancer cells. *Folia Histochem Cytobiol* 2008;46:315–321.
  37. Selvaggi G, Novello S, Torri V, et al. Epidermal growth factor receptor overexpression correlates with a poor prognosis in completely resected non-small-cell lung cancer. *Ann Oncol* 2004;15:28–32.
  38. Hirsch FR, Varella-Garcia M, Bunn PA Jr, et al. Epidermal growth factor receptor in non-small-cell lung carcinomas: correlation between gene copy number and protein expression and impact on prognosis. *J Clin Oncol* 2003;21:3798–3807.
  39. Shigematsu H, Lin L, Takahashi T, et al. Clinical and biological features associated with epidermal growth factor receptor gene mutations in lung cancers. *J Natl Cancer Inst* 2005;97:339–346.
  40. Gautschi O, Ratschiller D, Gugger M, et al. Cyclin D1 in non-small cell lung cancer: a key driver of malignant transformation. *Lung Cancer* 2007;55:1–14.
  41. Marchetti A, Doglioni C, Barbareschi M, et al. Cyclin D1 and retinoblastoma susceptibility gene alterations in non-small cell lung cancer. *Int J Cancer* 1998;75:187–192.
  42. Betticher DC, Heighway J, Hasleton PS, et al. Prognostic significance of CCND1 (cyclin D1) overexpression in primary resected non-small-cell lung cancer. *Br J Cancer* 1996;73:294–300.
  43. Jiang W, Kahn SM, Tomita N, et al. Amplification and expression of the human cyclin D gene in esophageal cancer. *Cancer Res* 1992;52:2980–2983.
  44. Gillett C, Fantl V, Smith R, et al. Amplification and overexpression of cyclin D1 in breast cancer detected by immunohistochemical staining. *Cancer Res* 1994;54:1812–1817.
  45. Kobayashi S, Shimamura T, Monti S, et al. Transcriptional profiling identifies cyclin D1 as a critical downstream effector of mutant epidermal growth factor receptor signaling. *Cancer Res* 2006;66:11389–11398.